Journal of Cerebral Blood Flow & Metabolism (2012) 32, 643–653

www.jcbfm.com

Vascular changes in rat hippocampus following a high saturated fat and cholesterol diet

Linnea R Freeman and Ann-Charlotte E Granholm

Department of Neurosciences and the Center on Aging, Medical University of South Carolina, Charleston, South Carolina, USA

The long-term effects of a diet rich in saturated fat and cholesterol on the hippocampus were evaluated in this study. It has previously been shown that this type of diet is detrimental to health, particularly affecting peripheral organs such as the heart and liver. However, effects on the brain have not been fully evaluated. This study focused on the hippocampus, a brain region instrumental for learning and memory and vulnerable to ischemic damage. Reduced blood–brain barrier (BBB) integrity and increased microgliosis were observed in the hippocampus of rats fed a high-saturated-fat and cholesterol (HFHC) diet for 6 months. Interestingly, an increase in hippocampal protein levels of occludin, a tight junction protein, was found in HFHC-treated rats as well. Further investigation revealed decreased expression of the occludin protein in blood vessels and increased expression in the dentate gyrus hilar neurons and mossy fibers of the hippocampal cornus ammonis 3 in HFHC-treated rats. Our results show alterations in BBB integrity and expression of tight junction proteins after long-term exposure to HFHC diet in rats. These findings may suggest a biologic mechanism for previously observed behavioral deficits occurring in rats fed this diet.
Journal of Cerebral Blood Flow & Metabolism (2012) **32,** 643–653; doi:10.1038/jcbfm.2011.168; published online 23 November 2011

Keywords: blood–brain barrier; diet; hippocampus; inflammation; neurodegeneration

Introduction

Diets high in saturated fat and cholesterol are damaging to peripheral organs such as the heart (i.e., cardiovascular disease), pancreas (i.e., type 2 diabetes), and liver (i.e., fatty liver disease) (Das, 2010). However, the mechanisms by which a diet high in saturated fat and cholesterol affects the brain are still poorly understood. Although many people consume this type of diet and do not experience a heart attack or stroke, it is possible that a poor diet produces damaging effects to the brain that go unnoticed until a later age, especially through vascular-related events. Previous studies on the effects of a high-fat and/or high-cholesterol (HFHC) diet have revealed various detrimental changes to the brain and behavior, including reduced hippocampal neurogenesis (Hwang *et al*, 2008), increased oxidative stress (Morrison *et al*, 2010), and altered microvascular pathology (Franciosi *et al*, 2009). Furthermore, high fat diet-induced obesity has been correlated with reduced focal gray matter volume and enlarged white matter in the frontal lobe (Pannacciulli *et al*, 2006), altered learning, memory, and executive function in humans (Elias *et al*, 2003) and cognitive deficits in a rodent model (Winocur and Greenwood, 2005).

The hippocampus is a central component in learning and memory behavior and it is one of the main regions affected in Alzheimer's disease (AD) (Marlatt and Lucassen, 2010). However, it is also an area of the brain that is particularly vulnerable to ischemic and/or hypoxic stroke. It is not fully understood why the hippocampus is a vulnerable area, but possible factors include its location and lack of vascularization (Nikonenko *et al*, 2009). Recent evidence connects AD with alterations to the blood–brain barrier (BBB) (Altman and Rutledge, 2010). Furthermore, elevations in blood cholesterol levels during middle age have the most profound effects on AD risk (Altman and Rutledge, 2010); therefore, providing a link between effects of a high-fat diet (increased serum cholesterol) with vascular and memory changes observed in the brain. It is not yet fully understood what occurs mechanistically during this time frame to increase the risk for neurodegeneration and AD. In a previous study from our laboratory, a HFHC diet (10% hydrogenated coconut oil with 2% added pure cholesterol) was administered to middle-aged rats for 8 weeks.

Correspondence: Dr LR Freeman, Department of Neurosciences, 411 Basic Science, 171 Ashley Avenue, Medical University of South Carolina, Charleston, SC 29425, USA.
E-mail: freemal@musc.edu
This study was supported the Nutrition Council of South Carolina and NIA Grants AG04418, F31AG033482.
Received 16 July 2011; revised 16 September 2011; accepted 24 October 2011; published online 23 November 2011

We found a significant impairment in performance on the water radial arm maze, which was correlated with reduced expression of the dendritic marker microtubule associated protein 2 (MAP2) in the hippocampus and elevated serum cholesterol levels for HFHC-treated rats (Granholm *et al*, 2008). This study focused on vascular changes after 6 months exposure to the HFHC diet in middle-aged rats. As clinical studies suggest that elevated cholesterol levels in mid-life predict age-related dementia (Kalmijn, 2000), it is possible the HFHC diet exacerbates the aging process leading to a greater degree of neurodegeneration and loss of BBB integrity but this has not been explored previously.

The BBB is a complex unit of endothelial cells 'glued' together with various proteins such as tight junction proteins (i.e., occludin and claudin), scaffolding proteins (i.e., ZO-1 and ZO-2), and astrocytes, which lend their end feet to create a system that selectively allows certain substances to reach the brain while keeping other substances out (del Zoppo and Mabuchi, 2003). Although it is known that cholesterol can form deposits within blood vessels in the periphery after consumption of a HFHC diet (Jensen *et al*, 2011), cholesterol does not cross the BBB and the brain synthesizes cholesterol *in situ* to be incorporated into cell membranes and myelin sheaths (Vance *et al*, 2006). However, it is possible that this obstruction occurs in the brain or at least alters cerebral vascularization. It has previously been shown that atherosclerosis in the aorta can lead to vascular inflammation in the brain, leading to neuronal dysfunction (Tibolla ;*et al*, 2010). Adding to this, cholesterol, saturated fat, and trans fat have proven to be damaging through increasing oxidative stress and inflammation (Uranga *et al*, 2010).

An important component of the BBB is occludin, an integral membrane protein found in endothelial cells (Lochhead *et al*, 2010). It has been shown to interact directly with numerous intracellular proteins. For example, occludin binds ZO-1, a scaffold molecule that also structurally supports the BBB (Fanning *et al*, 1998), and itch, a ubiquitin-protein ligase, which has suggested a mechanism for its role in protein trafficking and degradation (Traweger *et al*, 2002). Furthermore, occludin interacts with enzymes, lipid kinases, and cytokines that alter tight junction assembly/disassembly (Aijaz *et al*, 2006; Furuse *et al*, 1993). It has also been shown in neurons, wherein its effects are not yet fully understood (Romanitan *et al*, 2010).

In this study, we analyzed blood vessel morphology, BBB integrity, occludin localization, and activated microglia within the hippocampus of female Fischer 344 rats. Rats were fed a control rat chow diet or hydrogenated coconut oil with added cholesterol (HFHC) for 6 months during middle age (rats started the diet at age 6 months and ended at 12 months). The aims of this study were two-fold: to analyze the potentially damaging effects of the HFHC diet on vascularization and to further explore changes to the BBB from the diet.

Materials and methods

Animals and Diets

Six-month-old female Fischer 344 rats (Harlan, Indianapolis, IN, USA) were given 1 week to acclimate to the vivarium and then randomly divided into two dietary groups ($n=6$ control group and $n=8$ treatment group). Animals were housed 2 to a cage and kept on a controlled 12-hour light/12-hour dark cycle with *ad libitum* access to food and water. The control diet consisted of standard rat chow (8656 Harlan Teklad Sterilizable Rodent Diet, Harlan). The treatment diet (HFHC) consisted of (by weight): 10% hydrogenated coconut oil and 2% cholesterol ('Custom Diet D2-AIN93 without choline bitartrate and with 2% cholesterol') manufactured by MP Biomedicals (Solon, OH, USA). Both diets contained the necessary vitamins and minerals for adult health. Rats were fed control or HFHC diet from the age of 6 to 12 months. Animal protocols were approved by the Medical University of South Carolina Institutional Care and Use Committee and carried out according to guidelines from the National Institutes on Health.

Body Weights and Food Consumption

Body weights (measured in grams) were evaluated every other week to monitor effects of the diet on weight. Food consumption was measured weekly per cage (two rats per cage) throughout the study and is expressed as grams per week per cage.

Serum Total Cholesterol and Triglyceride Levels

Rats were killed with isoflurane gas (Novaplus, Irving, TX, USA), the chest was opened, and blood was collected through cardiac puncture. Blood was allowed to clot for at least 2 hours, and then centrifuged to collect serum which was stored at -20°C until analysis. Serum cholesterol and triglyceride (TG) levels were analyzed using the Synchron Systems kit (Beckman Coulter, Brea, CA, USA) as described previously (Granholm *et al*, 2008). The CHOL reagent was used to measure cholesterol concentration by a timed-end point method. In the reaction, cholesterol esterase hydrolyzes cholesterol esters to free cholesterol and fatty acids. Free cholesterol was oxidized to cholestene-3-one and hydrogen peroxide by cholesterol oxidase. Peroxidase catalyzed the reaction of hydrogen peroxide with 4-aminoantipyrine and phenol to produce a colored quinoneimine product. The Synchron System automatically proportioned the appropriate sample and reagent volumes into the cuvette. The ratio used was 1 part sample to 100 parts reagent. The system monitors the change in absorbance at 520 nm. This change in absorbance is directly proportional to the concentration of CHOL in the sample and is used to calculate and express CHOL concentration. Triglycerides glycerophosphate oxidase reagent (Synchron) was used to

measure the TG serum concentration by a timed-end point method. Triglycerides in the sample were hydrolyzed to glycerol and free fatty acids by the action of lipase. A sequence of three coupled enzymatic steps using glycerol kinase, glycerophosphate oxidase, and horseradish peroxidase causes the oxidative coupling of 3,5-dicholor-2-hydroxybenzenesulfonic acid with 4-aminoantipyrine to form a red quinoneimine dye. The Synchron System automatically proportions the appropriate sample and reagent volumes into the cuvette. The ratio used is 1 part sample to 100 parts reagent. The system monitors the change in absorbance at 520nm. This change in absorbance is directly proportional to the concentration of TG in the sample and is used to calculate and express TG concentration.

Morphologic Evaluation of the Hippocampus

Animals were killed with an overdose of isofluorane (Novaplus) and their brains rapidly removed. The right hemisphere was immersion fixed in 4% paraformaldehyde for 48 hours and then transferred to 30% sucrose prepared in 0.1 mol/L phosphate-buffered saline (PBS) for later morphologic analysis. The hippocampus was dissected from the left hemisphere and flash frozen for biochemical analysis.

The right hemisphere was sectioned on a cryostat (Zeiss-Microm, Thornwood, NY, USA) to a thickness of 40 μm through the hippocampus and the sections were kept free floating in phosphate buffer. Immunofluorescence was performed on serial sections (every twelfth section) using the following antibodies: SMI-71 (rat blood–brain barrier, Covance, Emeryville, CA, USA, concentration 1:100), Glut-1 (glucose transporter 1, Chemicon, Billerica, MA, USA, concentration 1:100), OX-6 (RT1B class II monomorphic for activated microglia, Serotec, Raleigh, NC, USA, concentration 1:100), and Occludin (Zymed Laboratories, San Francisco, CA, USA, concentration 1:100). Sections were washed in PBS and incubated in primary antibody overnight at 4°C. Sections were then washed in PBS, incubated with secondary antibody conjugated to Alexa-Fluor 488 or Alexa-Fluor 594 (Molecular Probes, Eugene, OR, USA) for 1 hour, washed again in PBS, and then coverslipped with PVA/DABCO (polyvinyl alcohol mounting medium with DABCO, anti-fading agent). Sections were visualized using a Nikon Optiphot fluorescence microscope equipped with a Nikon camera (Nikon, Melville, NY, USA). To better visualize SMI-71-ir (as shown in Figures 2D to 2F and 2J to 2L), microscopy with a Fluoview500 Olympus confocal microscope (Olympus Fluoview, Tokyo, Japan) was used with the appropriate band-pass filter for Alexa-Fluor 594 (sequential scans).

Evaluation of Occludin Antibody

To test the specificity of the occludin antibody, a pre-absorption control experiment was performed using the occludin immunogen (Zymed Laboratories). The immunogen was incubated at a 10-fold dilution (1:10) with the antibody 24 hours before immunohistochemistry was performed. The experiment was executed using the same protocol as described above for occludin (dilution 1:100). The only changes for this experiment included the use of the primary antibody that had already been incubated with its immunogen, and a positive control in which a primary antibody without the immunogen was used.

Densitometry

Semiquantification of immunofluorescence on hippocampal sections was performed with a periodicity of every twelfth section through the hippocampus. A Nikon Optiphot fluorescence microscope equipped with a Nikon camera using a 10 $\times$ lens was used to capture images of the hippocampus and adjacent cortex. Images were then converted to black and white for densitometry experiments. Using Nikon Elements Image Software (NIS Elements, Melville, NY, USA), analysis was performed blinded, at least three sections per rat were measured, and values from the images were averaged to obtain a mean per animal value. The region of interest for each section (i.e., CA1 of the hippocampus) was outlined and the software assigned a value based on a grayscale level where white = 0 and black = 256 for the given area measurements. Mean intensity values were averaged per animal, compared between groups, and then analyzed for statistical significance using the StatView software (Statview Version 5.0.1, SAS Institute, Cary, NC, USA) as described previously (Granholm *et al*, 2008).

Semiquantification of microgliosis was also performed by hand counting OX-6-immunoreactive cells in the hippocampus, using a systematic random design. Cell counts were performed blinded using a Nikon Optiphot fluorescence microscope equipped with a Nikon camera and NIS Elements software to visualize OX-6 positive cells. A 10 $\times$ objective was used to visualize the hippocampus for cell counts. At least three sections per animal were evaluated, with a randomized start section and a set periodicity thereafter to avoid counting the same profile twice. Cells outside the gray matter of the hippocampus were not counted (i.e., fimbria/fornix region). As stereology cell counting requires a sample size of at least 100 profiles per brain (Gundersen *et al*, 1988), it was not possible to use this unbiased method for OX-6-immunoreactive profiles.

Western Blot

The left hippocampus was rapidly dissected, frozen on dry ice in preweighed Eppendorf tubes, and then kept at −80°C until western blot analysis was performed. Lysis buffer (containing NP-40 and SDS with protease and phosphatase inhibitors) was added to each sample and then samples were homogenized using a pestle and 20-G needle and syringe. The supernatant and pellet were separated by spinning samples at 4°C at 14,000 r.p.m. for 20 minutes. The supernatant was used for this study. A bicinchoninic acid protein assay was used to calculate total protein within the supernatant samples. NuPAGE Bis-Tris (4 to 12%) gels were loaded with 20 μg protein for occludin and ZO-1 experiments. For occludin, gels were run with NuPAGE MES Buffer, and for ZO-1, gels were run with NuPAGE MOPS Buffer. Gels were transferred onto

nitrocellulose, and ZO-1 experiments used a transfer buffer with added SDS and decreased methanol because of the large protein size, 225 kDa. Blots were incubated with 5% instant milk suspended in PBS with 0.1% Tween 20. Next, blots were incubated with the primary antibody Occludin (Zymed Laboratories, 1:125) or ZO-1 (Zymed Laboratories, 1:125) overnight at 4°C. After incubation with the primary antibody, blots were washed and incubated with the secondary antibody (horseradish peroxidase-tagged goat anti-rabbit, 1:5,000). Blots were washed again and then developed using a chemiluminescent reagent (1:1 dilution of Immobilon). After development and visualization, blots were analyzed for band density using the FluorChem 9900 software (Cell Biosciences, Santa Clara, CA, USA).

Statistical Analysis

Data are represented as mean ± s.e.m. Statistical analysis was performed using an unpaired *t*-test to determine whether there were significant differences in body weights, food consumption, TG, and total cholesterol levels between the two treatment groups (significance was set at $P < 0.05$). An unpaired *t*-test was also used to analyze densitometry results from immunofluorescent experiments and western blotting experiments. Pearson's correlation matrix was used to determine whether linear relationships existed between the different markers.

Results

Body Weights and Food Consumption

The HFHC-treated rats consumed significantly more food than did control animals, when examining average food consumption per week over the 6-month diet treatment ($P = 0.0005$, control = 164 ± 3 ($n = 3$ cages, 5 animals), HFHC = 179 ± 3 ($n = 4$ cages, 8 animals); Figure 1A). In addition, rats that received the HFHC diet weighed significantly more at the end of the 6-month period ($P < 0.0001$) than did rats fed the control diet (control = 213 ± 5 ($n = 5$ animals), HFHC = 239 ± 2 ($n = 8$ animals); Figure 1B).

Triglyceride and Cholesterol Levels

Serum was collected from each rat at the time of killing to determine fasting TG levels and total cholesterol levels after 6 months of exposure to their particular diet. Rats that received the HFHC diet exhibited significantly elevated serum cholesterol levels ($P = 0.0003$) than did the control group (control = 76.2 ± 0.6 ($n = 5$ animals), HFHC = 115 ± 6 ($n = 8$ animals); Figure 1C). There were no significant differences observed for fasting TG levels between the HFHC and control groups at the end of the 6-month treatment ($P = 0.5551$, control = 243 ± 35

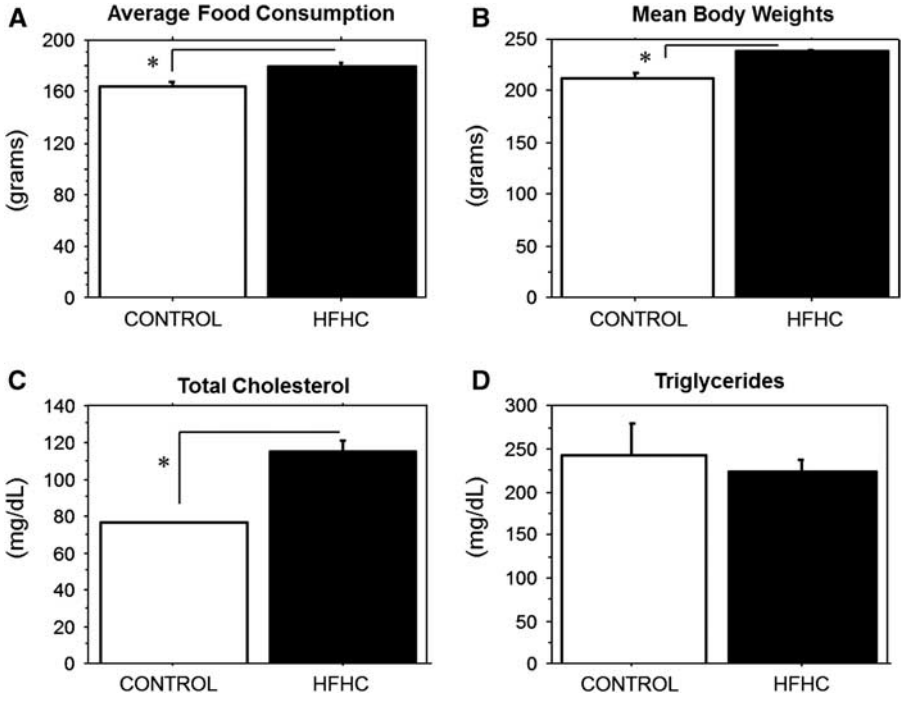

Figure 1 (**A** to **D**). Food consumption, mean body weights, total cholesterol, triglycerides. (**A**) HFHC-treated animals consumed more food than did control animals ($P = 0.0005$). (**B**) The HFHC-treated group was significantly heavier on average at the end of the experiment ($P < 0.0001$) than the control group. (**C**) The HFHC-treated group exhibited significantly elevated serum cholesterol levels ($P = 0.0003$) than did with the control group. (**D**) No significant differences were observed for fasting triglyceride levels between the HFHC and control groups ($P = 0.5551$). HFHC, high-fat/high cholesterol. The asterisks in **A**–**C** denotes highly significant differences ($P < 0.001$).

($n = 5$ animals), HFHC = 224 ± 14 ($n = 8$ animals); Figure 1D).

Blood–Brain Barrier Integrity as Measured by SMI-71

Immunofluorescence was performed on serial sections throughout the hippocampus using the antibody SMI-71 (an antibody specific to the rat endothelial-barrier protein, EBA). Figure 2 displays representative images for SMI-71 immunofluorescence in the CA1, CA3, and cortex of HFHC diet and control-fed rats. Images were captured at 10 × (Figures 2A to 2C and 2G to 2I) and converted to grayscale using NIS Elements (Nikon). Mean density data are presented to the right of the images for the particular region (Figures 2M to 2O). Figures 2D to 2F and 2J to 2L display images captured on the confocal microscope (Olympus Fluoview) with a 60 × objective. A single vessel was captured and a *z*-stack was produced to visualize SMI-71 immunoreactivity within the vascular wall. Immunoreactivity in the vascular wall was greatest for both groups in the CA3 region of the hippocampus, whereas the cortex displayed more tightly packed and a greater number of vessels compared with the CA1 and CA3. Control rats exhibited robust SMI-71 immunoreactivity that was well distributed throughout each region of interest. Conversely, HFHC-treated rats had reduced immunoreactivity in the CA1 and cortex. This overall reduction was evident in the 10 × images as less vessels exhibited SMI-71 immunoreactivity, and the 60 × confocal images revealed punctate immunoreactivity along the individual vessel walls. Punctate immunoreactivity may be attributed to a loss in tight junction protein expression or a conformational change of the protein(s). This has been shown previously by Lochhead *et al* (2010) and McCaffrey *et al* (2008, 2009), as their experiments using stress induced by hypoxia or hyperalgesia resulted in a reorganization of occludin, changes to occludin trafficking, and increased BBB permeability. A systematic random design was developed to evaluate differences in mean density of immunoreactivity within the CA1, CA3, and the adjacent section of the parietal cortex for SMI-71 immunoreactivity, to confirm observed differences in SMI-71 staining density. A significant decrease in immunoreactivity was observed in the CA1 region for HFHC diet-fed rats than in controls ($P = 0.0363$, control = 97 ± 18 ($n = 5$ animals), HFHC = 55 ± 8 ($n = 8$ animals); Figure 2M), as well as the cortex ($P = 0.0222$, control = 155 ± 22 ($n = 5$ animals), HFHC = 97 ± 11 ($n = 8$ animals); Figure 2O). However, no significant differences were observed between the groups in the CA3 region ($P = 0.7806$, control = 116 ± 25 ($n = 5$ animals), HFHC = 109 ± 11 ($n = 8$ animals); Figure 2N), confirming a regional loss of SMI-71 expression particularly evident in the hippocampal CA1 region and the overlying parietal cortex.

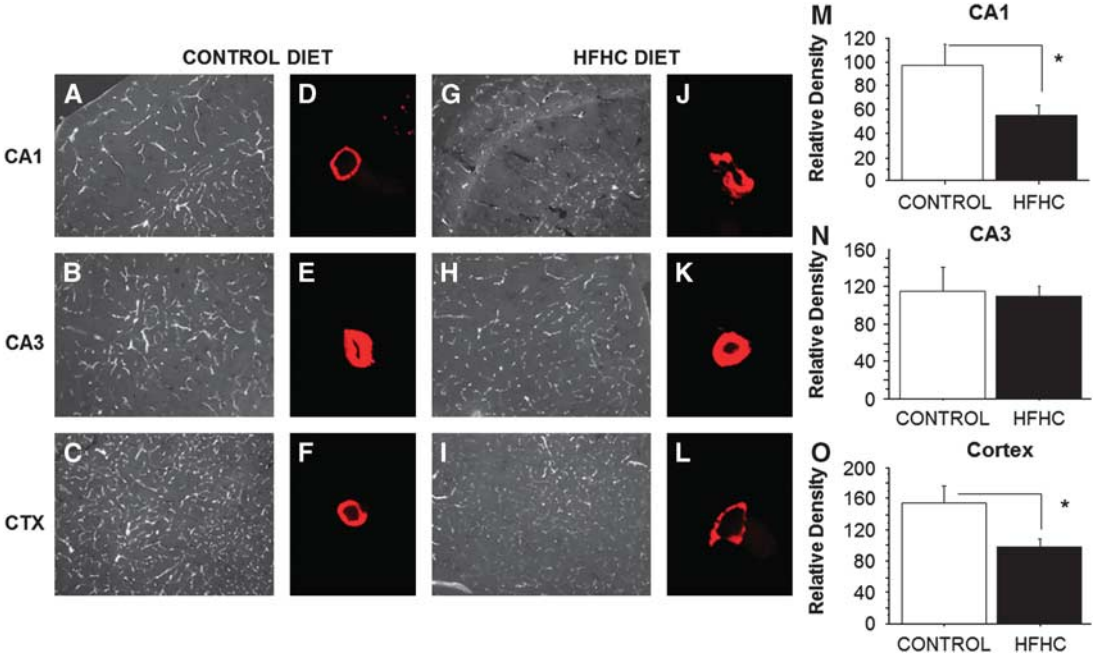

Figure 2 Blood–brain barrier integrity as measured by SMI-71. Images were captured at 10 × (**A** to **C** and **G** to **I**) and converted to grayscale using NIS Elements. Mean density data are presented to the right of the images for the particular region (**M** to **O**). (**D** to **F** and **J** to **L**) displays images captured on the confocal microscope with a 60 × objective. A significant decrease in immunoreactivity was observed in the CA1 region for HFHC diet-fed animals compared with control ($P = 0.0363$), as well as the cortex ($P = 0.0222$). However, there were no significant differences observed in the CA3 region ($P = 0.7806$). Scale bar shown in panel **I** = 100 μm. HFHC, high-fat/high cholesterol. The asterisks in **M** and **O** denotes significant differences ($P < 0.05$).

Blood Vessel Morphology as Measured by Glut-1

Immunofluorescence was performed on serial sections throughout the hippocampus using the antibody Glut-1 (an antibody specific to glucose transporter 1). A systematic random design was again used to evaluate differences in the mean density of immunoreactivity within the CA1, CA3, and the overlying parietal cortex for the Glut-1 antibody. No significant differences in Glut-1 staining density were observed in any of these regions, including the CA1 ($P = 0.9408$, control = 64 ± 4 ($n = 5$ animals), HFHC = 65 ± 5 ($n = 8$ animals)), the CA3 ($P = 0.9222$, control = 76 ± 6, HFHC = 76 ± 4 ($n = 8$ animals)), or the overlying parietal cortex ($P = 0.5968$, control = 75 ± 4 ($n = 5$ animals), HFHC = 77 ± 23 ($n = 8$ animals)) between HFHC and control-fed animals. Data are not shown because no distribution differences were observed using this marker.

Western Blot Analysis of Occludin and ZO-1

To examine whether BBB-related proteins were also altered by the HFHC diet, western blotting was used to quantify components of the BBB including occludin, a tight junction protein, and ZO-1, a tight junction scaffold protein in the hippocampus. Band density was determined as the background subtracted from the occludin or ZO-1 band of interest divided by the background subtracted from the β-actin band (the loading control for this experiment). Data are reported as percentage of average control. Contrary to our hypothesis, HFHC-treated animals displayed a significant increase in occludin protein levels in the hippocampal homogenates ($P = 0.0243$, control = 1.3 ± 0.25 ($n = 5$ animals), HFHC = 2.4 ± 0.45 ($n = 7$ animals)) compared with controls (Figure 3A). Conversely, no significant differences were found in the hippocampus for the ZO-1 protein levels between control and HFHC-treated groups ($P = 0.7534$, Figure 3B). These findings might suggest a compensatory upregulation of occludin protein levels as a result of the long-term HFHC diet treatment.

Occludin Immunoreactivity

To examine tissue distribution of occludin in different cell types and structures in the hippocampus, occludin immunofluorescence was performed. Images in Figure 4 reveal occludin immunoreactivity in vessels (top), mossy fiber axons (middle), as well as the dentate gyrus hilar region (bottom). The same antibody used for western blotting was used for this immunofluorescence experiment. Occludin immunoreactivity was more dense in control blood vessel walls (Figure 4A) compared with HFHC-treated vessels (Figure 4B). Conversely, occludin immunoreactivity was greater in HFHC-treated mossy fiber axons and dentate gyrus cells in the hilar region for HFHC rats (Figure 4D) than in control rats (Figure 4C). As shown at the top of the figure, the section from the control rat revealed punctate immunoreactivity along the vessel, but it was tightly packed throughout with high intensity. The HFHC-treated rat also exhibited punctate occludin immunoreactivity, but it was not as intense throughout the vessel as the control. It should also be noted in this image for the HFHC animal (Figure 4B), that fibers around the vessel displayed immunoreactivity that was not nearly as prevalent in controls (Figure 4A). These mossy fibers from the CA3 region are shown more clearly in Figures 4C and 4D and show denser and higher-intensity immunoreactivity for HFHC-treated rats. Finally, both control and HFHC-treated rats displayed occludin immunoreactivity in the dentate gyrus hilar region. However, as was shown in the mossy fibers, higher-intensity immunoreactivity was found in the HFHC-treated group.

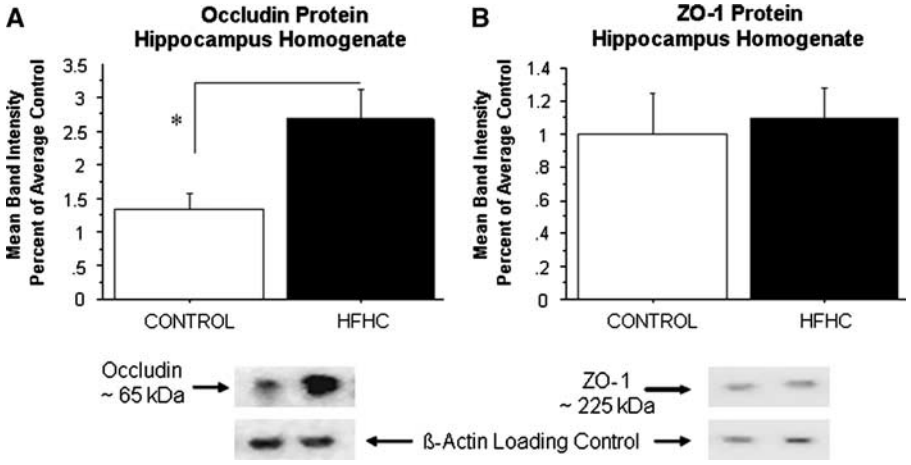

Figure 3 Western blot analysis of occludin and ZO-1. (**A**) HFHC-treated rats displayed a significant increase in hippocampal occludin protein expression ($P = 0.0243$) compared with control. (**B**) No significant differences were found for the ZO-1 protein between control and HFHC-treated groups ($P = 0.7534$). HFHC, high-fat/high cholesterol. The asterisk in **A** denotes a significant difference ($P < 0.05$).

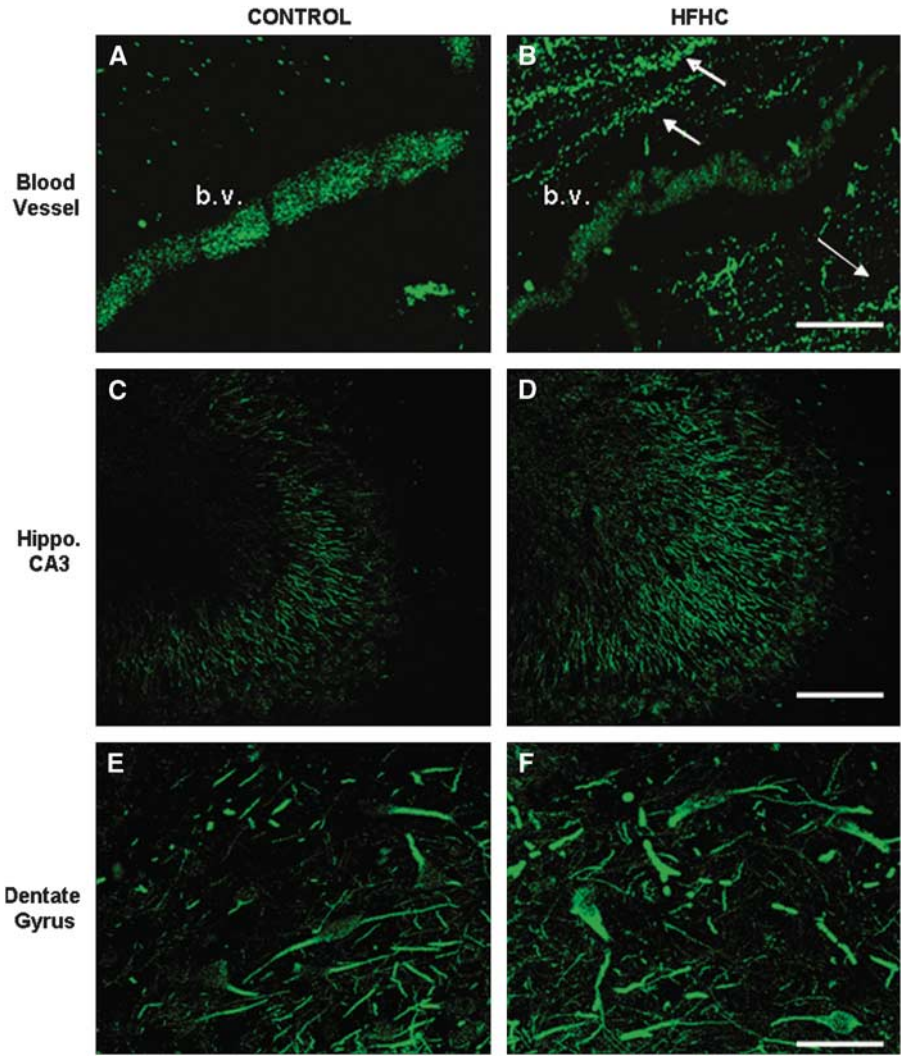

Figure 4 Occludin immunoreactivity. Occludin immunoreactivity is shown in vessels (**A** and **B**), mossy fiber axons (**C** and **D**), as well as in dentate gyrus granule cells (**E** and **F**). The same antibody used for western blotting was used for this immunofluorescence experiment. Occludin immunoreactivity was more dense in the control blood vessel compared with the HFHC-treated vessel, but was elevated in mossy fiber axons and dentate gyrus granule cells compared with control animals. Scale bars shown in panels **B** and **F** = 100μm. Scale bar shown in panel **D** = 200μm. White arrows in panel **B** indicate occludin expression in mossy fiber axons. HFHC, high-fat/high cholesterol.

A preabsorption control experiment revealed a lack of immunoreactivity showing specificity of the antibody to the antigen.

OX-6 Labeling of Microglial Cells

Immunohistochemistry was performed on serial sections throughout the hippocampus using the antibody OX-6, a major histocompatibility complex class II marker, to evaluate the number of activated microglial cells in the two groups. Figures 5A to 5C display images from the hippocampus captured at 20$\times$ for control and HFHC-fed rats, respectively. Semiquantitation by hand counting OX-6-positive cells revealed a significant increase in HFHC-treated rats than in control rats (Figure 5D). The majority of activated microglial cells were found in the CA3 region of the hippocampus close to the fimbria/fornix. Very few cells were found in the CA1 region, and none were found in the dentate gyrus in any of the groups. Although control rats exhibited a few activated microglial cells, they were typically found alone and at a distance from other activated microglia in that section. The microglia themselves also had less intense immunoreactivity both in the cell body and their processes, longer processes, and a smaller cell body compared with those found in HFHC-treated animals as displayed in Figure 5. Not only were there greater numbers of activated microglia in the HFCHC-treated animal's hippocampus, but the microglia were also found in clusters,

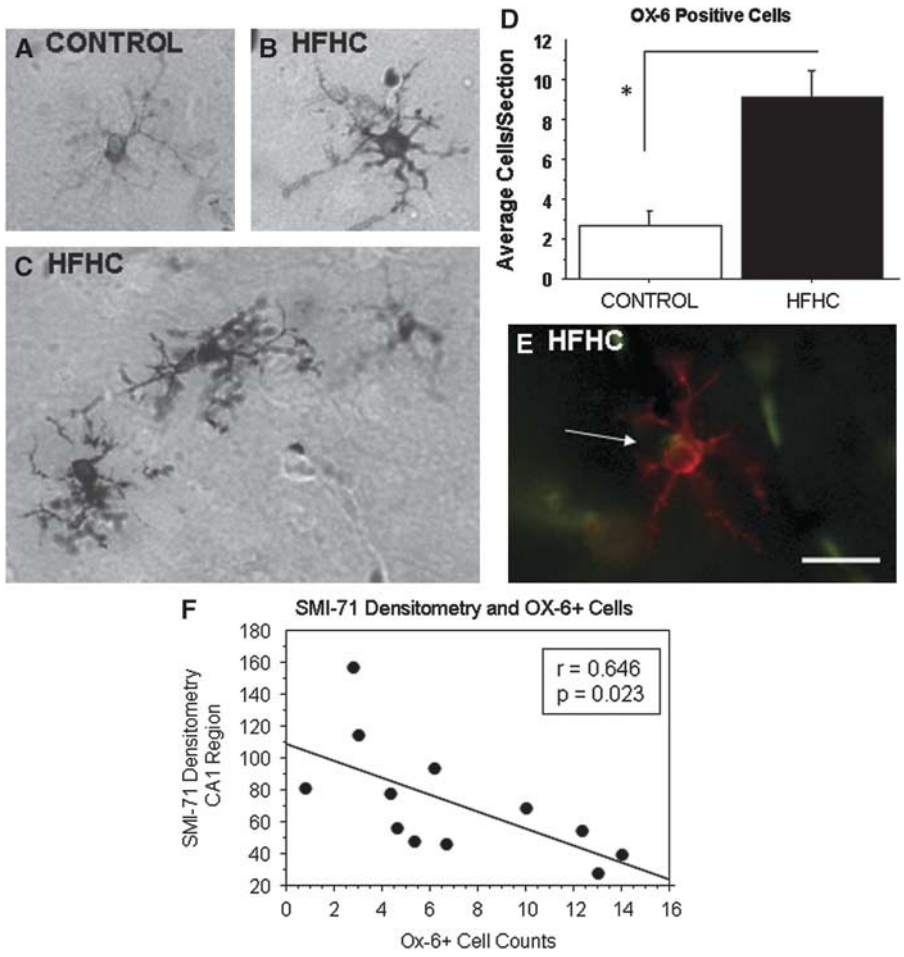

Figure 5 OX-6 immunoreactivity. Semiquantitation of OX-6-positive cells revealed a significant increase in the HFHC-treated group than in the control group. Images from the hippocampus were captured at $\times 20$ for (**A**) control and (**B** and **C**) HFHC-fed animals. (**D**) Cell counts per animal (3 to 5 sections analyzed per animal) were averaged and the average cell counts per treatment group were determined. (**E**) Most notable, the activated microglia were typically found on or close to blood vessels. (**F**) Furthermore, OX-6-positive cell counts were correlated with SMI-71 immunoreactivity in the CA1 region of the hippocampus. This observation points to a potential connection between microgliosis and vascular changes in the study. Scale bar shown in panel **E** = 50 μm. White arrow in panel **E** points to overlap of OX-6-ir (red, microglia) and Glut-1-ir (green, blood vessel), indicating a possible interaction between the two. HFHC, high-fat/high cholesterol.

displayed large cell bodies, and intense immunoreactivity throughout the cell body and processes, suggesting a marked elevation of OX-6 expression intracellularly. Most notable, the activated microglia were typically found on or close to blood vessels (Figure 5E). As shown in Figure 5F, the number of OX-6-positive cells was correlated with SMI-71 immunoreactivity in the CA1 region of the hippocampus. An increased number of OX-6-positive cells revealed reduced SMI-71 immunoreactivity. This observation points to a potential connection between inflammation and vascular changes in this study.

Discussion

We investigated the effects of an HFHC diet on vascularization, BBB integrity, and the number of activated microglia in the hippocampus of middle-aged Fischer 344 rats. To our knowledge, previous studies have not investigated vascular changes in the brain as a result of long-term treatment with this type of diet in rats. The primary findings included a significant increase in serum cholesterol, a significant decrease in SMI-71 immunoreactivity in the CA1 and cortex, decreased occludin immunoreactivity on blood vessels, but increased immunoreactivity in mossy fiber axons and dentate gyrus granule cells, and a significant increase in microgliosis for those rats treated with the HFHC diet compared with control.

Six months of exposure to the HFHC diet led to a significant increase in body weight compared with rats treated with the control diet. The HFHC diet used here delivers $\sim$45% of calories from fat compared with 13% of calories from fat for the control diet. On the basis of the elevated caloric

intake, it is not surprising that the HFHC diet led to an increase in total body weights. However, in our previous dietary studies, weight gain and food consumption were not significantly different between groups (Granholm *et al*, 2008). We hypothesize that this difference may be caused by longer exposure to the diet (6 months in this study versus 8 weeks in previous studies) and the use of a lower fat control diet in this study. Although our previous studies did not lead to increased body weights or food consumption with the high-fat diet, they did reveal significantly increased serum cholesterol levels. Data from this study are consistent with those previous findings, and we propose that higher serum cholesterol is a potential factor for changes to vascularization in the brain. In the periphery, increased levels of cholesterol and oxidized low-density lipoprotein can deposit in vessels leading to occlusion and inflammation (Jensen *et al*, 2011). Although a direct mechanism has not been shown to date, recent studies have found a link between hypercholesterolemia and altered central nervous system microvascular pathology (Franciosi *et al*, 2009), as well as a link between a hyperlipidemic diet and altered microvascular morphology (Constantinescu *et al*, 2011). We hypothesize that increased serum cholesterol and inflammation are the main contributors to the deficits we are reporting here at the BBB.

Results from the SMI-71 immunofluorescence experiment point to a possible disruption of the BBB for HFHC-treated animals. The SMI-71 antibody has been used in other recent studies to evaluate BBB integrity (Katsu *et al*, 2010; Sheen *et al*, 2011). It is possible there is a loss in tight junction protein expression or there is an altered conformation of these proteins, which would contribute to a leaky BBB. As shown previously by Lochhead *et al* (2010) and McCaffrey *et al* (2008, 2009), hypoxia and peripheral inflammatory hyperalgesia led to notable changes for the critically important tight junction protein, occludin. The observed changes included a loss of disulfide bond integrity and reduced oligomeric assembly, which led to a subsequent loss in protein–lipid interactions and tight junction trafficking (Lochhead *et al*, 2010; McCaffrey *et al*, 2008, 2009). Additional studies on cerebral ischemia have also revealed a change in the localization of tight junction proteins coupled with paracellular permeability (Bangsow *et al*, 2008; Kago *et al*, 2006; Witt *et al*, 2003). Therefore, our results displaying reduced SMI-71 and occludin protein immunoreactivity on blood vessels may indicate a loss in tight junction protein and a consequent increase in BBB permeability at those sites. Many researchers have shown that BBB integrity is reduced because of aging itself and is linked to AD and other dementias (Altman and Rutledge, 2010; Deane and Zlokovic, 2007). Here, we provide data that a high-saturated-fat and cholesterol diet is another factor that could contribute to breakdown of the BBB.

To further examine BBB-related components following the HFHC diet, we measured hippocampal protein levels of occludin and ZO-1. Changes to occludin protein levels were intriguing because they revealed opposite results to our hypothesis: increased protein expression for HFHC-treated animals. However, with further investigation, we found that occludin immunoreactivity was reduced in blood vessel walls but increased in mossy fiber axons and in dentate gyrus hilar neurons for HFHC-treated animals. Further studies must be performed to elucidate the functional significance of this altered distribution of occludin. However, our observation of neuronal occludin expression is consistent with previous findings in the current literature. For example, human brain studies by Romanitan *et al* (2007, 2010) found expression of occludin and claudin family proteins (Cl-2,5,11) in neurons, astrocytes, and oligodendrocytes for aged control, AD, and vascular dementia brains. Interestingly, an upregulation of occludin and claudin family proteins was found for the AD and vascular dementia brains compared with controls. The authors proposed a role for claudin proteins and occludin in neuronal structures as a protective response to the vascular damage occurring in AD and vascular dementia (Romanitan *et al*, 2007, 2010). Occludin expression has also been found in neurons and astrocytes in the mouse brain in which the protein was detected in primary and secondary cultures by reverse transcriptase-PCR, western blotting, and immunofluorescence experiments. Low levels of expression were found in differentiated neurons and astrocytes compared with the higher levels found in undifferentiated, early-stage cells, and it was therefore concluded that occludin expression is dependent on the stage of development (Bauer *et al*, 1999). However, as we have shown and with the data collected by Romanitan *et al*, it is possible that occludin expression is elevated in the brain as a compensatory/protective response mechanism after injury. Another hypothesis for the role of occludin upregulation is that neurons regulate the synthesis and distribution of occludin in brain capillary endothelial cells (Schiera *et al*, 2003). Collectively, our data suggest that occludin is not only expressed in endothelial cells but also in neurons; the upregulation of occludin protein in HFHC-fed rats may be a response to vascular damage occurring from the HFHC diet.

Finally, a significant increase in the number of activated microglia was observed in the hippocampus of rats fed the HFHC diet compared with control rats. This is consistent with previous findings from our laboratory where we found increased microglial activation in middle-aged male rats treated with the HFHC diet (Freeman *et al*, 2011; Granholm *et al*, 2008). Activated microglial cells also have an important role in altering vascularization and the integrity of the BBB (Hawkins and Davis, 2005). A recent study revealed that lipopolysaccharide stimulation used to activate microglial cells led to

breakdown of the BBB through damage to endothelial cells (Kacimi *et al*, 2011). When cell culture experiments were performed without the presence of microglia, no damage to endothelial cells was observed suggesting an important role for these cells (Kacimi *et al*, 2011), most likely because of their ability to increase expression and release of proinflammatory cytokines.

In conclusion, we investigated the effects of a diet rich in saturated fat and cholesterol on vascularization and BBB integrity in the middle-aged female rat. The major findings of this study include: (1) the HFHC diet reduced SMI-71-ir (a BBB marker) in the hippocampus and the overlying parietal cortex, (2) the HFHC diet increased the number of activated microglia in the hippocampus, and (3) occludin protein expression was elevated in neurons and mossy fibers of the CA3 suggesting a compensatory upregulation of this protein.

Disclosure/conflict of interest

The authors declare no conflict of interest.

References

Aijaz S, Balda MS, Matter K (2006) Tight junctions: molecular architecture and function. *Int Rev Cytol* 248:261–98

Altman R, Rutledge JC (2010) The vascular contribution to Alzheimer's disease. *Clin Sci (Lond)* 119:407–21

Bangsow T, Baumann E, Bangsow C, Jaeger MH, Pelzer B, Gruhn P, Wolf S, von Melchner H, Stanimirovic DB (2008) The epithelial membrane protein 1 is a novel tight junction protein of the blood-brain barrier. *J Cereb Blood Flow Metab* 28:1249–60

Bauer H, Stelzhammer W, Fuchs R, Weiger TM, Danninger C, Probst G, Krizbai IA (1999) Astrocytes and neurons express the tight junction-specific protein occludin *in vitro*. *Exp Cell Res* 250:434–8

Constantinescu E, Safciuc F, Sima AV (2011) A hyperlipidemic diet induces structural changes in cerebral blood vessels. *Curr Neurovasc Res* 8:131–44

Das UN (2010) Obesity: genes, brain, gut, and environment. *Nutrition* 26:459–73

Deane R, Zlokovic BV (2007) Role of the blood-brain barrier in the pathogenesis of Alzheimer's disease. *Curr Alzheimer Res* 4:191–7

del Zoppo GJ, Mabuchi T (2003) Cerebral microvessel responses to focal ischemia. *J Cereb Blood Flow Metab* 23:879–94

Elias MF, Elias PK, Sullivan LM, Wolf PA, D'Agostino RB (2003) Lower cognitive function in the presence of obesity and hypertension: the Framingham heart study. *Int J Obes Relat Metab Disord* 27:260–8

Fanning AS, Jameson BJ, Jesaitis LA, Anderson JM (1998) The tight junction protein ZO-1 establishes a link between the transmembrane protein occludin and the actin cytoskeleton. *J Biol Chem* 273:29745–53

Franciosi S, Gama Sosa MA, English DF, Oler E, Oung T, Janssen WG, De Gasperi R, Schmeidler J, Dickstein DL, Schmitz C, Gandy S, Hof PR, Buxbaum JD, Elder GA (2009) Novel cerebrovascular pathology in mice fed a high cholesterol diet. *Mol Neurodegener* 4:42

Freeman LR, Haley-Zitlin V, Stevens C, Granholm AC (2011) Diet-induced effects on neuronal and glial elements in the middle-aged rat hippocampus. *Nutr Neurosci* 14:32–44

Furuse M, Hirase T, Itoh M, Nagafuchi A, Yonemura S, Tsukita S, Tsukita S (1993) Occludin: a novel integral membrane protein localizing at tight junctions. *J Cell Biol* 123:1777–88

Granholm AC, Bimonte-Nelson HA, Moore AB, Nelson ME, Freeman LR, Sambamurti K (2008) Effects of a saturated fat and high cholesterol diet on memory and hippocampal morphology in the middle-aged rat. *J Alzheimers Dis* 14:133–45

Gundersen HJ, Bagger P, Bendtsen TF, Evans SM, Korbo L, Marcussen N, Moller A, Nielsen K, Nyengaard JR, Pakkenberg B (1988) The new stereological tools: disector, fractionator, nucleator and point sampled intercepts and their use in pathological research and diagnosis. *APMIS* 96:857–81

Hawkins BT, Davis TP (2005) The blood-brain barrier/neurovascular unit in health and disease. *Pharmacol Rev* 57:173–85

Hwang IK, Kim IY, Kim DW, Yoo KY, Kim YN, Yi SS, Won MH, Lee IS, Yoon YS, Seong JK (2008) Strain-specific differences in cell proliferation and differentiation in the dentate gyrus of C57BL/6N and C3H/HeN mice fed a high fat diet. *Brain Res* 1241:1–6

Jensen TW, Mazur MJ, Pettigew JE, Perez-Mendoza VG, Zachary J, Schook LB (2011) A cloned pig model for examining atherosclerosis induced by high fat, high cholesterol diets. *Anim Biotechnol* 21:179–87

Kacimi R, Giffard RG, Yenari MA (2011) Endotoxin-activated microglia injure brain derived endothelial cells via NF-kappaB, JAK-STAT and JNK stress kinase pathways. *J Inflamm (Lond)* 8:7

Kago T, Takagi N, Date I, Takenaga Y, Takagi K, Takeo S (2006) Cerebral ischemia enhances tyrosine phosphorylation of occludin in brain capillaries. *Biochem Biophys Res Commun* 339:1197–203

Kalmijn S (2000) Fatty acid intake and the risk of dementia and cognitive decline: a review of clinical and epidemiological studies. *J Nutr Health Aging* 4:202–7

Katsu M, Niizuma K, Yoshioka H, Okami N, Sakata H, Chan PH (2010) Hemoglobin-induced oxidative stress contributes to matrix metalloproteinase activation and blood-brain barrier dysfunction *in vivo*. *J Cereb Blood Flow Metab* 30:1939–50

Lochhead JJ, McCaffrey G, Quigley CE, Finch J, DeMarco KM, Nametz N, Davis TP (2010) Oxidative stress increases blood-brain barrier permeability and induces alterations in occludin during hypoxia-reoxygenation. *J Cereb Blood Flow Metab* 30:1625–36

Marlatt MW, Lucassen PJ (2010) Neurogenesis and Alzheimer's disease: biology and pathophysiology in mice and men. *Curr Alzheimer Res* 7:113–25

McCaffrey G, Seelbach MJ, Staatz WD, Nametz N, Quigley C, Campos CR, Brooks TA, Davis TP (2008) Occludin oligomeric assembly at tight junctions of the blood-brain barrier is disrupted by peripheral inflammatory hyperalgesia. *J Neurochem* 106:2395–409

McCaffrey G, Willis CL, Staatz WD, Nametz N, Quigley CA, Hom S, Lochhead JJ, Davis TP (2009) Occludin oligomeric assemblies at tight junctions of the blood-brain barrier are altered by hypoxia and reoxygenation stress. *J Neurochem* 110:58–71

Morrison CD, Pistell PJ, Ingram DK, Johnson WD, Liu Y, Fernandez-Kim SO, White CL, Purpera MN, Uranga RM, Bruce-Keller AJ, Keller JN (2010) High fat diet increases hippocampal oxidative stress and cognitive impairment in aged mice: implications for decreased Nrf2 signaling. *J Neurochem* 114:1581–9

Nikonenko AG, Radenovic L, Andjus PR, Skibo GG (2009) Structural features of ischemic damage in the hippocampus. *Anat Rec (Hoboken)* 292:1914–21

Pannacciulli N, Del Parigi A, Chen K, Le DS, Reiman EM, Tataranni PA (2006) Brain abnormalities in human obesity: a voxel-based morphometric study. *Neuroimage* 31:1419–25

Romanitan MO, Popescu BO, Spulber S, Bajenaru O, Popescu LM, Winblad B, Bogdanovic N (2010) Altered expression of claudin family proteins in Alzheimer's disease and vascular dementia brains. *J Cell Mol Med* 14:1088–100

Romanitan MO, Popescu BO, Winblad B, Bajenaru OA, Bogdanovic N (2007) Occludin is overexpressed in Alzheimer's disease and vascular dementia. *J Cell Mol Med* 11:569–79

Schiera G, Bono E, Raffa MP, Gallo A, Pitarresi GL, Di Liegro I, Savettieri G (2003) Synergistic effects of neurons and astrocytes on the differentiation of brain capillary endothelial cells in culture. *J Cell Mol Med* 7:165–70

Sheen SH, Kim JE, Ryu HJ, Yang Y, Choi KC, Kang TC (2011) Decrease in dystrophin expression prior to disruption of brain-blood barrier within the rat piriform cortex following status epilepticus. *Brain Res* 1369: 173–83

Tibolla G, Norata GD, Meda C, Arnaboldi L, Uboldi P, Piazza F, Ferrarese C, Corsini A, Maggi A, Vegeto E, Catapano AL (2010) Increased atherosclerosis and vascular inflammation in APP transgenic mice with apolipoprotein E deficiency. *Atherosclerosis* 210:78–87

Traweger A, Fang D, Liu YC, Stelzhammer W, Krizbai IA, Fresser F, Bauer HC, Bauer H (2002) The tight junction-specific protein occludin is a functional target of the E3 ubiquitin-protein ligase itch. *J Biol Chem* 277:10201–8

Uranga RM, Bruce-Keller AJ, Morrison CD, Fernandez-Kim SO, Ebenezer PJ, Zhang L, Dasuri K, Keller JN (2010) Intersection between metabolic dysfunction, high fat diet consumption, and brain aging. *J Neurochem* 114:344–61

Vance JE, Karten B, Hayashi H (2006) Lipid dynamics in neurons. *Biochem Soc Trans* 34:399–403

Winocur G, Greenwood CE (2005) Studies of the effects of high fat diets on cognitive function in a rat model. *Neurobiol Aging* 26(Suppl 1):46–9

Witt KA, Mark KS, Hom S, Davis TP (2003) Effects of hypoxia-reoxygenation on rat blood-brain barrier permeability and tight junctional protein expression. *Am J Physiol Heart Circ Physiol* 285:H2820–31